

FORMATION OF SELF-ASSEMBLED NANOMETER-SCALE InP ISLANDS ON SILICON SUBSTRATES

A.S. Bakin*, D. Piester*, H.-H. Wehmann*, A.A. Ivanov*,
A. Schlachetzki*, K.D. Becker**

*Institut für Halbleitertechnik, Technische Universität Braunschweig, Hans-Sommer-Straße 66, D-38106 Braunschweig, Germany; e-mail: A.Bakin@tu-bs.de

**Institut für Festkörperchemie, Abteilung Physikalische Chemie, Technische Universität Braunschweig, Hans-Sommer-Straße 10, D-38106 Braunschweig, Germany

ABSTRACT

Three-dimensional islands of InP have been reproducibly grown in the Stranski-Krastanow growth mode on Si (001) and (111) by using metal-organic vapor phase epitaxy in order to obtain nanometer-scale quantum dots. Atomic-force microscopy was used to determine the morphology of the samples and to evaluate the dimensions of the islands. Formation of three-dimensional islands with densities as high as $2.5 \times 10^{10} \text{ cm}^{-2}$ and small sizes have been observed. The evolution of island morphology is explained in terms of strain-relaxing mechanisms at the first stages of InP/Si heteroepitaxy.

INTRODUCTION

Self-assembled nanometer-scale structures are at present topics of considerable interest due to their potential in optoelectronic and electronic device application and due to their process-unaaffected and damage-free features [1-9]. Supporting this statement is the experimental finding with InSb dots on InP substrates that Lomer-type of dislocations form a 90° grid at the substrate-island interface relaxing the mechanical tensions within the islands [1]. Thus we can expect that the bulk of the islands is defect-free as demonstrated by InAs dots on InP [4, 9]. The heterostructures of direct-band gap materials like InP on indirect-band gap silicon have the potential for a new generation of optoelectronic devices monolithically integrated with silicon-based microelectronics. This will ultimately lead to the fabrication of light sources on silicon. It is the intention of this paper to study the experimental conditions required for the formation of InP dots on Si substrates. Very little has been published on such islands. The knowledge of optimized growth conditions is essential for an effective control of the dot size.

The growth was performed in a horizontal infrared-heated metal-organic vapor phase epitaxy (MOVPE) machine designed by AIXTRON and operated at low pressure (20 to 100 hPa) under a total hydrogen flow of 8 l/min. Prior to growth the wet-chemically cleaned Si substrates were thermally treated at 950°C for 15 min in a hydrogen atmosphere in order to remove the native oxide. AsH_3 is introduced during the cool-down phase and then growth was started at 400°C [10, 11].

The effect of annealing of the samples was investigated by heating them up to a temperature of 640°C in a phosphine flow. After reaching 640°C the heater was immediately shut off. An atomic-force microscope (AFM) made by TopoMetrix was employed for the characterization of the structures.

Figures 1 a to f show AFM images selected from a series of samples obtained for different growth durations from 2 to 30 seconds on (001)Si substrates. Statistical data on the InP islands are given in Table 1.

Examples of the histograms of the island-height distribution are shown in Fig. 2. Such results form the basis for a statistical evaluation by a fit to a Gaussian distribution function as shown by the curves in Fig. 2. Most of the islands are of approximately the same geometry. The average density of the self-organized islands increases with the growth duration and attaining a saturation value of $2.5 \times 10^{10} \text{ cm}^{-2}$ after 4 s (Fig. 3).

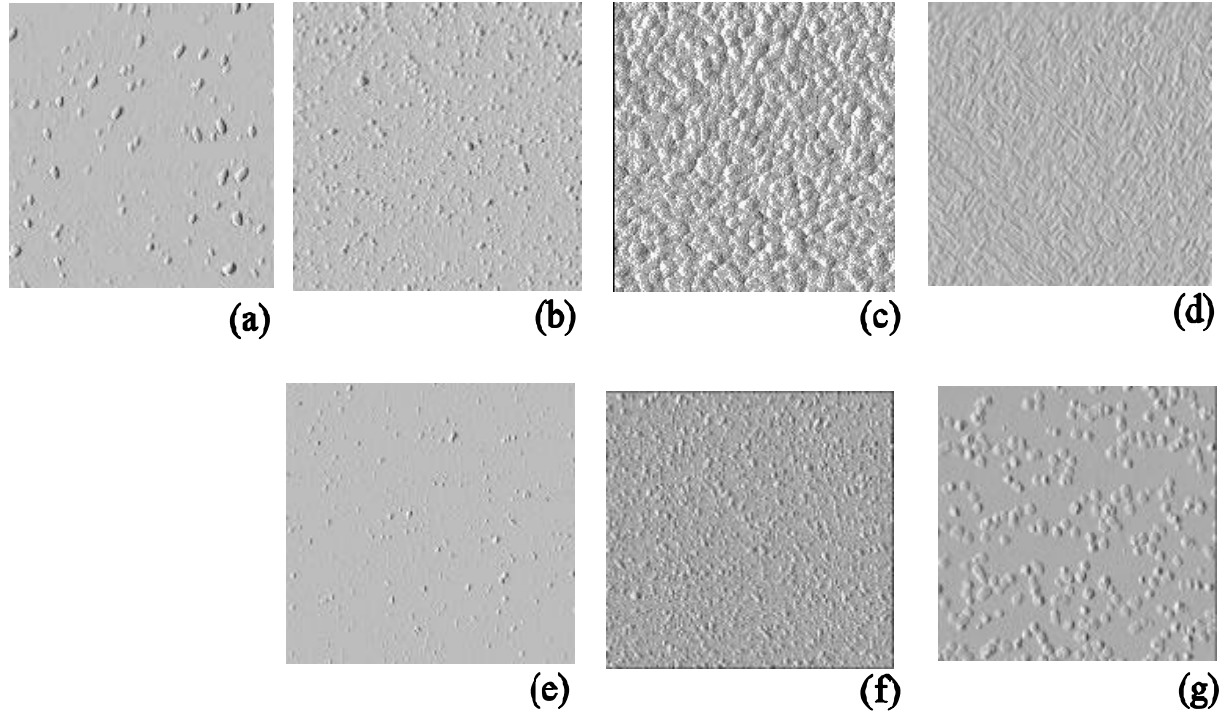


Fig. 1. AFM images ($2 \times 2 \mu\text{m}^2$ each) of self-organized InP islands on (001)Si for different growth durations, as-grown: a-2 s, b-4 s, c-15s, d-30 s, e-4 s (annealed), f-15 s (annealed), g-30 s (on Si(111));

Table 1. Statistical data of InP islands on (001)Si

Growth Duration (s)	As-grown			After annealing		
	Average height (nm)	Variance (nm^2)	Average density (cm^{-2})	Average height (nm)	Variance (nm^2)	Average density (cm^{-2})
2	29	4	5×10^9			
3	14.5	0.36	1.5×10^{10}	12.9	1.21	5×10^9
4	9	0.526	2.5×10^{10}	7	1.0	1.8×10^{10}
8	9.2	0.64	2.5×10^{10}	7	1.4	1×10^{10}
15	14	0.25	3×10^{10}			1.5×10^{10}

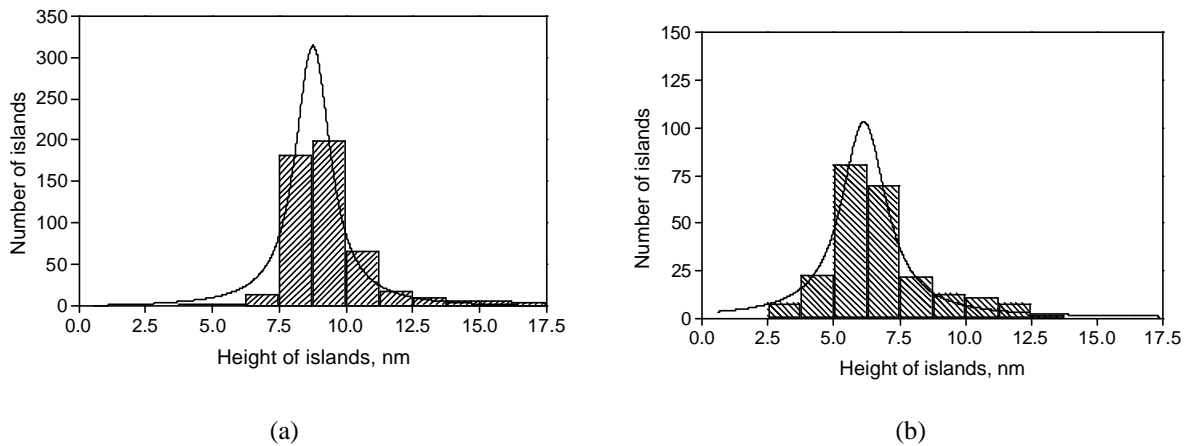


Fig. 2. Height distribution of InP islands on Si(100)
 a – as-grown islands (4s, cf. Fig 1b)
 b – after annealing (4s, cf. Fig 1e).

High densities of islands according to Stranski-Krastanow growth mode are explained by the fact that the InP/Si heterostructure is highly strained due to a lattice mismatch of about 8%. The strain energy in the "layer" is reduced because the 3D-islands can partly elastically relieve in contrast to a blanket layer. Such island formation is commonly observed with mismatched systems like SiGe/Si[7] and InAs/Si [8, 9].

The area- and the size-distributions depend on the growth duration, i.e. the total amount of deposited InP. Two growth modes can be distinguished: the initial-growth mode and the main-growth mode. During the initial mode, in our case up to about 4s, the size and the height of the islands decreases as the total amount of deposited InP rises, whereas their density increases (cf. Fig. 3).

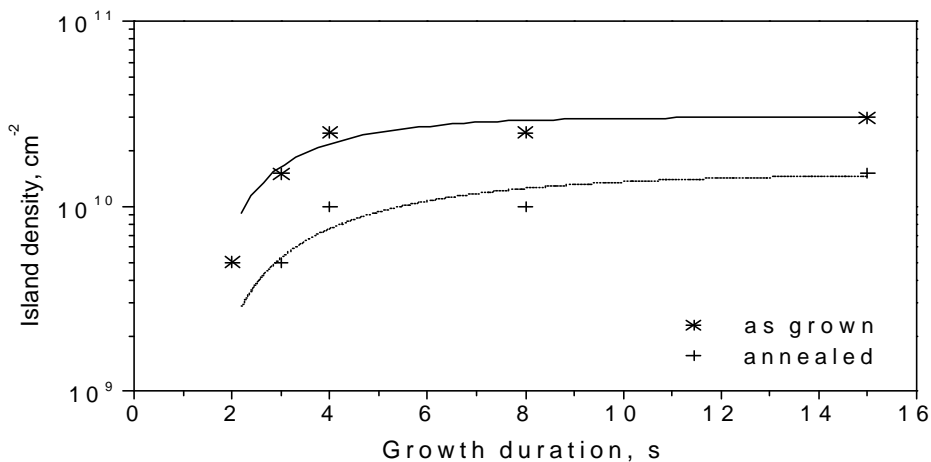


Fig. 3. Dependence of the island density on the growth duration on (001)Si substrates for as-grown samples (* and solid curve) and after the temperature increase up to 640°C (+ and dashed curve). The curves are given as a guide for the eye.

A decrease in island size while increasing the total amount of deposited material was also reported for InAs/GaAs [12, 13] and InAs/InP [14]. The surface diffusion length is large enough to permit the formation of islands separated by more than 300 nm for 2 to 3 s growth duration (cf. Fig. 1a). Despite the assumption that the largest coherent islands should be the most stable, the kinetics of the growth process inhibits the formation of large islands and promotes the nucleation of a greater number of small islands (Fig. 1b). However, not only the islands are strained but also the substrate below the islands is under tensile strain and consequently under compressive strain between the islands. The substrate distortion contributes to the strain relaxation and favors the island-growth mode. At the initial stage (2 s, 3 s) the islands are independent of each other since the active range of the strain field induced by each island is well below the distance to its neighbors. Depositing more InP causes an increase in island density (cf. Fig. 3). This is also demonstrated by a comparison of Fig. 1a and b. The maximum size of the islands remains essentially constant. This suggests that the size is limited not only by surface transport, otherwise, longer growth would lead to larger islands. After nucleation at a random place on the surface which is not affected by the strain field of already existing islands, the newly formed island may grow or again dissolve unless it reaches a critical size, which more or less corresponds to an optimum of the elastic relaxation [14]. Above this optimum the island is stable. However, there is also an upper limit in size which is given by the generation of a first misfit dislocation. After reaching this size the growth of an additional island will be energetically more favorable since the inhibiting effect of the compressive stress in the substrate next to the islands is missing. The initial growth mode (2 to 3 s) represents the behavior of coherent islands isolated from each other on the substrate. When the InP coverage increases the nucleation of islands continues and the distance to the next island will reach the interaction value. This leads to partial compensation of substrate distortion. Large islands become less favored. The islands assume smaller sizes with reduced interaction distance. Such self-organization occurs locally in places where the distance between islands falls below the critical value. During further InP-growth the increase in the surface coverage leads to an increase in island density. These are the characteristic features of the main growth mode after which the islands coalesce to a blanket film.

For growth durations of 15 s or more the AFM investigations revealed a partial coalescence of islands and after 30 s a complete coverage of the substrate (Fig. 1c, d). The surface of the forming layer becomes smoother, thus lowering the surface energy.

We studied the influence of the annealing treatment on the reorganization of the initial islands. The surface of the samples after annealing (i.e. heating up to 640°C and cooling under PH₃ flow) exhibits smaller, elongated islands with lower density and a larger size spread due to surface diffusion and evaporation (see Table 1 or Fig. 2b). Examples of the dot distribution after annealing is shown in Fig. 1e, f. These investigations are important for those cases when further growth should occur at subsequent hightemperature steps. Fig. 3 summarizes the results of our experiments.

A second point of interest is the island morphology. The cross-sections of two typical islands as seen by AFM are shown in Fig. 4. Most of the islands with dimensions larger than 30 nm are significantly anisotropic. The dots appear elongated in one of the two <010> directions of the Si substrate. This phenomenon can explain the formation of antiphase domains during further islands growth and coalescence [10, 15]. In Fig. 1d it is clearly seen that after coalescence areas with two different orientations were formed. As we have discussed previously, two kinds of coherent islands exist: first, large islands with flat top surface independent on each other and originating from random nucleation; and second, self-organized islands formed during the main growth, whose distribution and size depend on long range interactions. The isolated islands of

the first type are about two times larger in area than the islands formed during the subsequent growth. From AFM measurements we can suppose that the side walls of the islands, both as-grown and after annealing, are {111} and {311}.

In addition we studied the growth of self-organized InP islands on (111)Si substrates (Fig. 1g). All self-organized islands are of comparable size (as with (001) orientation). As compared to the growth on (001)Si the maximum density of the islands is slightly lower ($5 \times 10^9 \text{ cm}^{-2}$), but as clearly seen from a comparison of Fig. 1d (growth on (001)Si) and Fig. 1g (on (111)Si), the islands already coalesced for the same growth time on (001)Si.

CONCLUSIONS

In conclusion, three-dimensional islands of InP have been reproducibly grown on Si substrates using MOVPE and have been characterized by AFM. The dots are of remarkably homogeneous distribution in size and shape with a greater size dispersion after annealing. The dots present a truncated pyramidal morphology with rectangular base. We found two types of coherent islands: first, large islands with flat upper surface independent on each other and originating from random nucleation at the beginning of the deposition, and second, self-organized islands formed during the main growth, whose distribution and size depend on long range interactions. Initially isolated islands are about two times larger in size than islands formed during the further growth. This observation shows that the stability of an island does not only depend on its elastic and surface energies, but also on substrate distortion and long range interaction between islands. These investigations prove that MOVPE growth provides excellent control of growth rates down to the nanometer scale. Thus we expect that self-assembled nanometer-scale InP islands obtained in the present work can be employed for integration of new optical devices on Si, for further advanced InP growth and as a self-assembled mask for nanoscale patterning of the silicon substrate.

ACKNOWLEDGEMENTS

This work has been funded by the Deutsche Forschungsgemeinschaft.

REFERENCES

1. J.C. Ferrer, F. Peiro, A. Cornet, and J.R. Morante, *Appl. Phys. Lett.* 69, 3887 (1996).
2. H. Omi and T. Ogino, *Appl. Phys. Lett.* 71, 2163 (1997).
3. D. Lacombe, A. Ponchet, S. Frechengués, V. Drouot, N. Bertru, B. Lambert, and A. Le Corre, *Appl. Phys. Lett.* 74, 1680 (1999).
4. H. Marchand, P. Desjardins, S. Guillon, J.-E. Paultre, Z. Bougrioua, R. Y.-F. Yip, and R.A. Masut, *Appl. Phys. Lett.* 71, 527 (1997).
5. M. Sönanen, H. Lipsanen and J. Ahopelto, *Appl. Phys. Lett.* 67, 3768 (1995).
6. B. Wang, F. Zhao, Y. Peng, Z. Jin, Y. Li, and S. Liu, *Appl. Phys. Lett.* 72, 2433 (1998).
7. J.S. Sullivan, H. Evans, D.E. Savage, M.R. Wilson, and M.G. Lagally, *J. Electron. Mater.* 28, 426 (1999).
8. H. Lee, W. Yang, P.C. Serce, and A.G. Norman, *J. Electron. Mater.* 28, 481 (1999).
9. P.C. Sharma, K.W. Alt, D.Y. Yeh, D. Wang, and K.L. Wang, *J. Electron. Mater.* 28, 432 (1999).

10. G.-P. Tang, Ph.D thesis, *Fortschritt-Berichte* 5/360, VDI Verlag, Düsseldorf, Germany, (1994).
11. A. Lubnow, Ph.D thesis, *Fortschritt-Berichte* 9/166, VDI Verlag, Düsseldorf, Germany, (1993).
12. J.M. Gerard, J.B. Genin, J. Lefebvre, J.M. Moison, N. Lebouche, and F. Barthe, *J.Cryst. Growth* 150, 351 (1995).
13. D. Leonard, K. Pond, and P.M. Petroff, *Phys. Rev. B* 50, 11687 (1994).
14. A. Ponchet, A. Le Corre, H.L Haridon, B. Lambert, and S. Salain, *Appl. Phys. Lett.* 67, 1850 (1995).
15. G.-P. Tang, A. Lubnow, H.-H. Wehmann, G. Zwinge and A. Schlachetzki, *Jpn. J. Appl. Phys.* 31, L1126 (1992).